Science Press

ARTICLE

Effect of Rare Earth(CeCl₃) on Oxidation Resistance of Ni₂Al₃/Ni Composite Coatings on Heat-resistant Steel

Zhao Yongtao[1],   Tian Zhihua[1],   Li Bobo[1],   Ren Huiping[2]

[1] Inner Mongolia University of Science and Technology, Baotou 014010, China; [2] Key Laboratory of Integrated Exploitation of Bayan Obo Multi-Metal Resources, Baotou 014010, China

Abstract: Ni-Al composite coatings were successfully prepared on the surface of P92 ferritic heat-resistant steel by electroplating nickel and low temperature packing cementation aluminum methods. The anti-oxidation experiment of the composite coating was carried out at 650 °C for 132 h. The microstructure of cross section, chemical element distribution and phase transformation of the coating before and after oxidation were characterized by OM, SEM, EDS and XRD. The results show that all the oxidation kinetics curves of the coatings are in accordance with the parabolic law. The average oxidation rate of the composite coating without Ce is 0.4412×10^{-6} g/(cm^2·s). In contrast, the average oxidation rate of the coating with 2 wt% CeCl$_3$ added in the aluminizing agent is 0.2957×10^{-6} g/(cm^2·s), which indicates that the oxidation resistance is obviously improved. However, the addition of excess CeCl$_3$ (4 wt%, 6 wt%) will produce more holes in the oxidation process and deteriorate the high-temperature oxidation resistance of the coating. In these cases, the oxidation rates of samples are higher than that of samples with 2 wt% CeCl$_3$ added. Moreover, the addition of Ce element in the coating increases the adhesion of the oxide film and has an inhibitory effect on the inward diffusion of the Al element.

Key words: Ni-Al coating; P92 steel; high temperature oxidation resistance; Ce; plating

The 9-12Cr (wt%) type ferritic heat-resistant steels are cheaper than austenitic heat-resistant steels and have higher creep limit. They have been widely used in superheater, reheater, water wall, header and steam pipe of ultra-supercritical thermal power units[1,2]. Compared with other ferritic heat-resistant steel, P92 steel has higher high-temperature strength and better creep properties. However, when the service temperature is above 650 °C, P92 steel cannot self-generate Cr$_2$O$_3$ film and its oxidation resistance will decrease sharply. By changing the composition or surface modification of such ferritic steel, it can be applied at higher steam temperatures, thereby increasing the thermal efficiency of steam turbine [3-6]. Among the three types of metal alloy protective coatings, i.e. Al$_2$O$_3$, Cr$_2$O$_3$ and SiO$_2$, Al$_2$O$_3$ has the most stable chemical properties in high temperature steam. Therefore, it is a potential method to improve the high temperature oxidation resistance of the ferritic heat resistant steel

via a self-generated alumina film by preparing an aluminum-rich alloy coating on the surface of the ferritic heat-resistant steel[7-9]. However, the lifetime of the coating is governed by the rate of inter-diffusion at the coating/steel matrix interface, which will cause oxide skin scaling as soon as the Al content falls to a critical level[10-12].

At present, researchers have successfully prepared a kind of Ni$_2$Al$_3$-Ni double layer composite coating. The outer layer of the coating is Ni$_2$Al$_3$, which provides oxidation resistance, and the inner layer is Ni, which plays a role in preventing the diffusion of Al towards the heat-resistant steel matrix[13,14]. It was reported that the Ni$_2$Al$_3$-Ni composite coating can maintain its structural stability at 650 °C for at least 11361 h[15,16]. Whereas, the inter-diffusion rate between the inner Ni layer and the matrix interface is too fast, which will affect the serviceability of the coating and reduce the creep strength of the component. Rare earth has great potential in the metal surface modifica-

tion. It has been confirmed that rare earth can play an important role in reinforcing the high temperature oxidation resistance of the material by catalyzing and promoting seepage in the coating, changing the morphology and properties of the second phase and refining the coating microstructure[17,18]. Xu et al[19] prepared aluminized coatings on Ti-based alloys with different Y contents by powder method and investigated the isothermal oxidation behaviors of coatings. It was found that the growth of the coatings is mainly controlled by the inner diffusion of Al. The addition of Y element can change the diffusion mechanism of Al, and reduce the oxidation rate of the aluminized coating significantly.

In this paper, a rare earth doped Ni-Al composite coating with moderate thickness and high density was prepared by doping rare earth Ce into the aluminizing agent to further improve its high temperature oxidation resistance. The effects of rare earth contents on the oxidation resistance properties of coatings at high temperature were investigated, and the mechanisms of the improvement of oxidation resistance of the coating were discussed accordingly.

1 Experiment

1.1 Experiment materials

The rare earth doped Ni-Al composite coatings were prepared on the surface of P92 ferritic heat-resistant steel by electroplating nickel and low temperature packing cementation aluminum methods. The P92 steel substrate composition was Fe-9Cr-1.8W-0.5Mo-0.1C (wt%). All surfaces of the samples (15 mm×12 mm×3 mm) were flattened by SiC sandpaper and polished afterwards.

The synthesis of the coating involved two steps. First nickel plating was performed in the traditional Watts liquid solution, and then the aluminum permeated at a low temperature (650 °C) for 8 h. Aluminizing agent consisted of aluminum powder, NH_4Cl, anhydrous $CeCl_3$, and the filler of 99.99% purity alumina particles. The specific composition of the aluminizing agent was $6Al-2NH_4Cl-xCeCl_3-(92-x)Al_2O_3$ (x=0, 2, 4, 6, wt%), and the corresponding sample is shown in Table 1. The actual Ce content of the prepared coating measured by ICP-MS is given in parenthesis. It can be seen that the higher the content of $CeCl_3$ added in the aluminizing agent, the higher the content of Ce in the coating.

After aluminizing, the samples were cleaned and weighed (sample+crucible) using an electronic balance with an accuracy of 10^{-5} g.

1.2 Oxidation tests

The oxidation experiments were carried out in a horizontal furnace at 650 °C for 132 h in air. The samples were taken out from the furnace at 24, 60, 96, and 132 h, successively. Then, mass gain (sample+crucible) was measured using the same electronic balance. In order to make the results accurate, three samples were used for each experiment to measure the average mass change.

1.3 Characterization

The actual Ce content of the prepared coating was measured using inductively coupled plasma mass spectrometry (ICP-MS). The cross-sectional microstructure of the rare earth added composite coating after oxidation was observed and analyzed by optical microscope (OM) (Axiovert25). The structure and composition were analyzed by scanning electron microscopy (SEM) (QUANTA400) with an energy dispersive X-ray spectroscopy (EDS) (Oxford INCA). By employing an X-ray diffraction (XRD) (D8ADVANCE with Cu-Kα source radiation), the phases of coating surface were characterized.

2 Results and Discussion

2.1 Characterization of the prepared Ni-Al coatings

According to our previous research[20], the thickness of nickel layer is controlled to about 100 μm for aluminizing, which can take advantage of activity restriction principle to suppress the mutual diffusion of elements and enhance the thermal stability of the coating. Fig.1 shows the cross-section morphologies of Ni-Al composite coatings with different $CeCl_3$ contents. It can be seen that the thickness of the aluminized layer of the sample 0# varies between 11~18 μm. The thickness of the aluminized layer of sample 1# varies between 21~23 μm and the coating surface is smooth without obvious defects. However, the surfaces of sample 2# and 3# are uneven and their aluminum layer thicknesses fluctuate around 20 μm. In particular, the surface of the penetrating layer of sample 3# shows a serious leakage phenomenon and the defects also increase significantly, which may cause a lot of looseness or even penetration layer spalling. It indicates that the proper amount of Ce can improve the coating quality and the addition of $CeCl_3$ in the aluminizing agent can promote osmosis acting as a catalyst.

Furthermore, XRD results (Fig.2) show that all the surface phases of prepared coatings consist of Ni_2Al_3 and a small quantity of Ni. The addition of rare earth does not change the surface phase composition of the coating. Due to the small content of Ce element, the XRD pattern cannot accurately determine the existence of its compound, as shown in Fig.2.

2.2 Oxidation kinetics curves of composite coatings at 650 °C

Fig.3a shows the mass gain per unit area ($\triangle M/A$, mg/cm^2) as a function of time after oxidation of the samples in air at

Table 1 Oxidation mass gain equation and oxidation rate of P92 steel Ni-Al composite coating

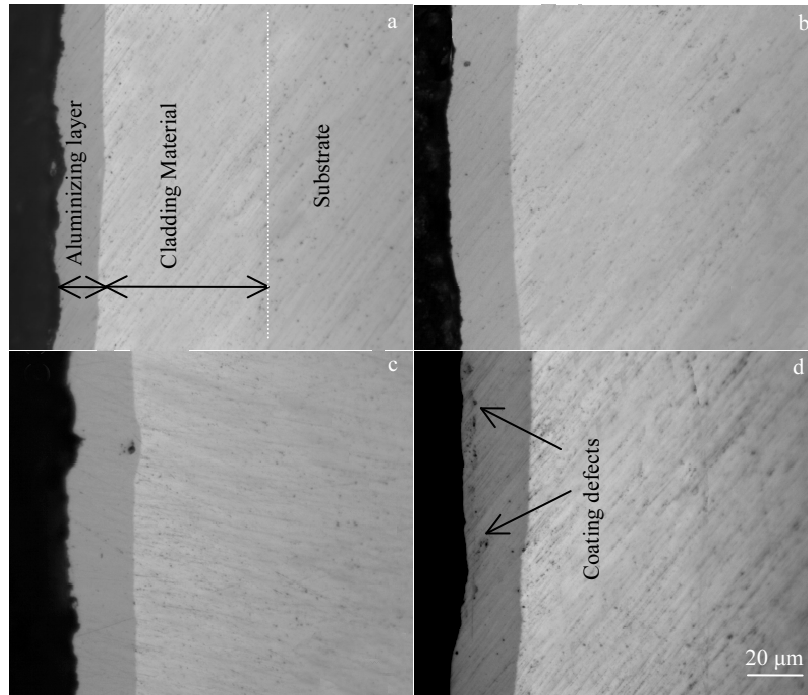| Sample	$CeCl_3$ /wt%	Square root fitting line equation	Average oxidation rate/×10^{-6} g·cm^{-2}·s^{-1}	Adj. R^2
0#	0 (0)	y=0.02647x−0.03397	0.4412	0.99961
1#	2 (0.08)	y=0.01774x−0.01028	0.2957	0.99109
2#	4 (0.1)	y=0.02137x−0.0368	0.3562	0.99053
3#	6 (0.13)	y=0.02120x−0.0181	0.3533	0.99838

Fig.1 Cross-sectional morphologies of prepared coatings: (a) 0#, 0 wt% CeCl$_3$, (b) 1#, 2 wt% CeCl$_3$, (c) 2#, 4 wt% CeCl$_3$, and (d) 3#, 6 wt% CeCl$_3$
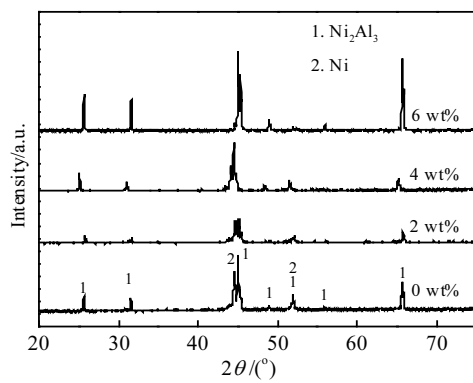

Fig.2 X-ray diffraction patterns of surface of the prepared coatings with different CeCl$_3$ contents
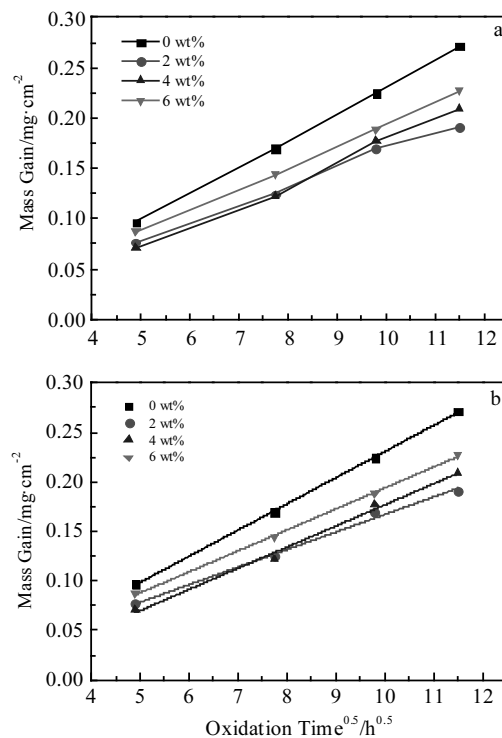

Fig.3 Oxidation kinetics curves (a) and fitting results (b) of rare earth added Ni-Al composite coating in air at 650 °C

650 °C. The oxidation kinetics curve after fitting is shown in Fig.3b. It is shown that the Adj. R^2 (adjusted coefficient of determination) values of fitted curves are all close to 1. This indicates that the fitting result is accurate. After oxidation at 650 °C for 132 h, as shown in Table 1, the oxidation mass gain equation and oxidation rate of the composite coating with different Ce contents are calculated. It can be seen that the fastest oxidation rate of the coating occurs in the composite coating of aluminizing agent without anhydrous CeCl$_3$ and its average value is about 0.4412×10^{-6} g/(cm^2·s). The coating with 2 wt% CeCl$_3$ addition in the aluminizing agent has the strongest

oxidation resistance and exhibits the optimal protection effect of 0.2957×10^{-6} g/(cm^2·s) oxidation rate. However, the average oxidation rate of 4 wt% CeCl$_3$ and 6 wt% CeCl$_3$ contained coating is 0.3562×10^{-6} and 0.3533×10^{-6} g/(cm^2·s), respectively. It reveals that an appropriate addition of CeCl$_3$ into aluminizing agent will enhance the oxidation resistance, but excessive addition of CeCl$_3$ will adversely affect the oxidation resistance.

According to the theory of parabolic growth kinetics proposed by Wagner[21], metal oxide parabolic law at high temperature is as follows:

$$y^n = kt + c \qquad (1)$$

where y is mass gain per unit area, t is oxidation time, n is index factor, and both k and c are constants. In the case of $n>2$, it is shown that the oxide film formed by this oxidation mode has a smaller retardation than the element diffusion. Meanwhile, the diffusion of ions forms a dense barrier layer that decreases the oxidation rate. When $n<2$, the oxide diffusion retardation is not directly proportional to the film thickness, and the characteristics of the oxide film including loose film and the existence of defects such as voids, stress and grain boundary diffusion may increase the oxidation rate. In the initial stage of oxidation, the oxide film formed on the coating surface prevents the corrosive gas such as oxygen from entering the coating and slows the oxidation rate. At the later stage of oxidation, a dense oxide film forms on the coating surface and the oxidation rate tends to be constant.

In this paper, the oxidation experiment of the coating was carried out in air at 650 °C. According to the oxidation kinetics curve and the fitting result, it is clear that n is equal to 2,

which is consistent with the law of parabola. With the increase of the oxidation time, the thickness of the oxide film gradually increases and the oxidation rate becomes smaller and smaller. The oxidation rate is negligible when a sufficiently thick oxide film is formed.

2.3 Cross-sectional morphologies of composite coatings after oxidation

The cross-sectional morphologies of samples after oxidation for 132 h are presented in Fig.4. It can be seen that there are a lot of holes, micro-cracks and other defects in the 0# sample, the oxide layer is loose, and intermittent peeling occurs. The sample 1# forms a small number of holes at the position of about 17 μm to the coating surface. The hole band of sample 2# is deeper and mainly distributed at the joint interface. In comparison, the number of holes in sample 3# obviously increases that almost connect each other to form cracks. At the same time, compared to sample 0#, the oxide films in the coating of 1#, 2# and 3# are thinner.

At high temperature, because the diffusion rate of aluminum from the aluminized layer to the pure nickel layer is greater than the diffusion rate of nickel from the pure nickel layer to the aluminized layer, the position where the concentration gradient of aluminum is the largest (interface between the aluminized layer and the pure nickel layer) will form a large number of voids due to the Kirkendall effect. In order to reduce energy, vacancies will inevitably gather into holes once formed[22]. With increasing the oxidation time, the holes further increase and accumulate until
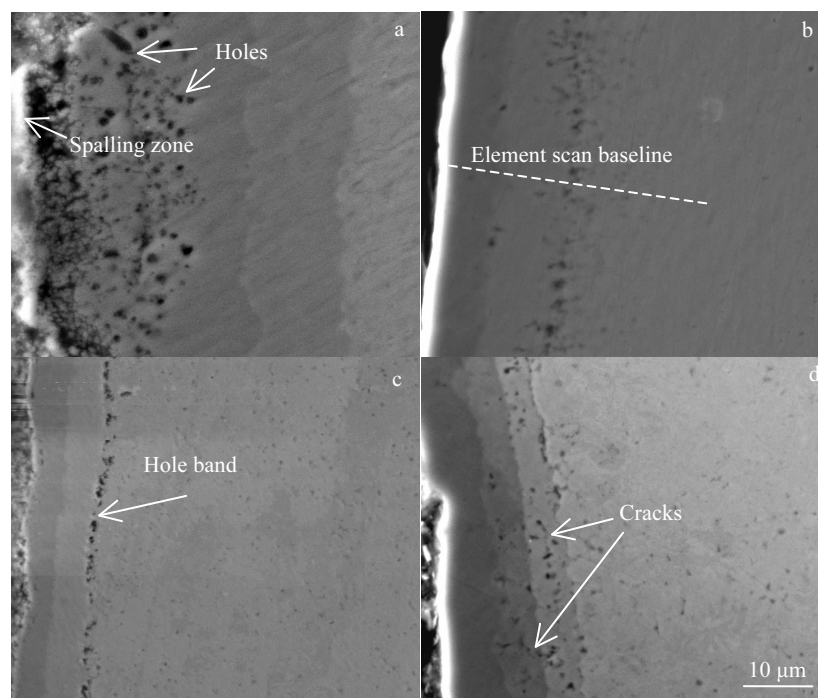

Fig.4   Cross-sectional morphologies of rare earth added Ni-Al composite coatings after oxidation at 650 °C for 132 h: (a) 0#, 0 wt% CeCl$_3$, (b) 1#, 2 wt% CeCl$_3$, (c) 2#, 4 wt% CeCl$_3$, and (d) 3#, 6 wt% CeCl$_3$

a linear crack forms. Therefore, in all four samples, holes appear at the interface between the aluminized layer and the pure nickel layer. However, the amount of holes in the interface of the 2# and 3# sample is obviously larger than in sample 1#. This may be due to the fact that an appropriate amount of Ce plays a role as "vacancy trap" in inhibiting the formation and aggregation of interfacial vacancies, while a large amount of Ce may form rare earth-containing compounds[23]. There is a possibility that the phase boundary and grain boundaries of these compounds can serve as a fast channel for Al diffusion instead of restraining vacancies. As a surface active element, Ce oxides preferentially form during oxidation and may become the nucleation site of Al_2O_3. Therefore, a uniform and complete oxide film forms rapidly on the surface of the coating due to the growth of Ce oxides being transformed into synergistic nucleation and growth with Ce-Al-O, such as $CeAlO_3$. Because of the barrier effect of the oxide film, not only the short-circuit diffusion channel of aluminum to the surface but also the inward migration of O atoms through the grain boundary of the oxide film is hindered, so that the aluminum oxide film always keeps thin status. Meanwhile, a proper amount of Ce-Al-O segregated in the grain boundary of Al_2O_3 acts as a pin suppressing grain growth at high temperature[24] and releases thermal stresses via increasing the diffusion creep of the fine grains. Therefore, the adhesion and anti-spalling properties of the oxide film are improved. As we can see, the thickness of the oxide film in all the samples with Ce addition is thinner than that of samples without Ce addition, and their surfaces have no obvious spalling.

2.4 Depth profiles of Al, Cr, Fe and Ni in the composite coatings

Fig.5 shows the depth profiles of alloy elements of samples after oxidation at 650 °C for 132 h (EDS scan baseline is shown in Fig.4b). It can be seen that the diffusion distance of Al element to the coating surface in 0#, 1#, 2# and 3# sample is 70~72, 38~41, 48~50 and 61~63 μm, respectively. It reveals that the addition of $CeCl_3$ in aluminizing agent can suppress the diffusion of Al in the coating. In addition, Fe and Cr elements are mainly enriched in the matrix, which proves that the Ni layer effectively blocks the diffusion of Al into the matrix and the diffusion of matrix elements into the aluminized layer, consistent with the original design of the double-layer composite coating. It can also be seen that Ce elements have little effect on the diffusion of Fe and Cr elements.

According to the calculation, the average diffusion rate of Al in 0# and 1# samples is 1×10^{-12} and 1×10^{-15} cm^2/s, respectively. And the diffusion rate of aluminum in sample 2# or 3# is between them. This is because Ce can affect the diffusion of elements inside the coatings during the oxidation process[25]. It is more difficult for Ce to diffuse in Ni[26] due to its higher diffusion activation energy in Ni. However,
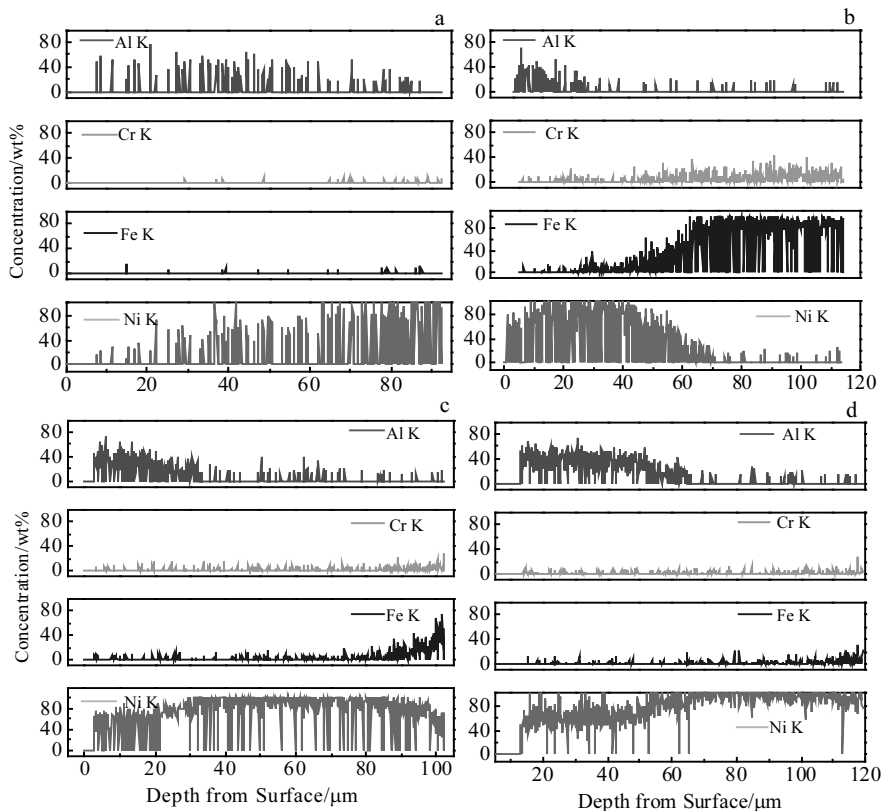

Fig.5   Depth profiles of Al, Cr, Fe and Ni in composite coatings after oxidation at 650 °C for 132 h: (a) 0#, 0 wt% $CeCl_3$, (b) 1#, 2 wt% $CeCl_3$, (c) 2#, 4 wt% $CeCl_3$, and (d) 3#, 6 wt% $CeCl_3$

the addition of Ce in coatings will affect the diffusion behavior of Al. Al diffuses in Ni mainly by the vacancy mechanism [27]. The large atomic size of Ce leads to its occupation in the normal lattice position and production of some vacancies in the Ni lattice. Thus, Ce dwindles the vacancy concentration in Ni and hinders Al atom to diffuse through the vacancy mechanism. As a result, the diffusion rate of Al decreases, such as sample 1#. However, excess Ce will seriously exceed the matrix's ability to dissolve them and form a large amount of Ce-containing compounds and mesophase. This will change nearby element concentration distribution, create more local defects, and promote short-circuit diffusion of Al. Subsequently, the oxidation resistance of the coating is deteriorated, such as sample 2# and 3#.

2.5 Phase changes in the coating oxidation process

Fig.6 shows surface X-ray diffraction pattern of sample 1# after oxidation at 650 °C for 132 h. With the sharp diffraction peak, XRD patterns confirm that the type of Al_2O_3 is γ-Al_2O_3. During the oxidation process, Al diffuses outward and the phase in coating surface transforms to Al-lean phase consequently. Therefore, a small amount of NiAl phase also appears on the sample surface. An Al_2O_3 oxide film forms firstly on the surface of the coating during oxidization in the air atmosphere, and it transfers from metastable θ-Al_2O_3 to metastable γ-Al_2O_3 during the following growth process. Since rare earth does not change the main phase transformation of the coating during the oxidation,

only 1# sample is used as an example. Fig.7 shows the EDS results of the sample 1# at a distance of about 10 μm from the surface of the coating after oxidation for 24, 60, 96 and 132 h. According to Table 2, the Ni-Al phase at 10 μm is Ni_2Al_3 at the beginning of oxidation and it partly transforms to NiAl at 60 h and completely converts to NiAl at 96 h. During the subsequent oxidation, the NiAl phase remains stable until 132 h without any phase change.

It has been reported that[28,29] below 854 °C, the order of Ni-Al phase formation is $NiAl_3 \rightarrow Ni_2Al_3 \rightarrow NiAl \rightarrow Ni_3Al$. In this paper, due to the short aluminizing time at the temperature of 650 °C and the limited heat accumulation, only $NiAl_3 \rightarrow Ni_2Al_3$ transformation occurs. When the coating was oxidized for 60 h, the phase change at a distance of 10
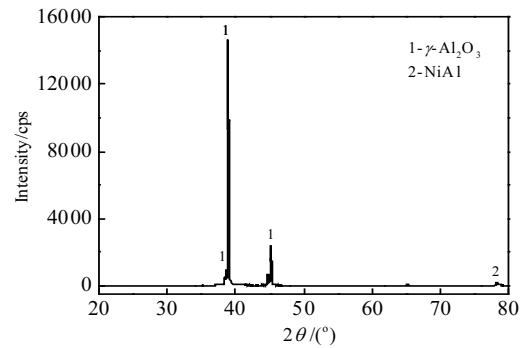
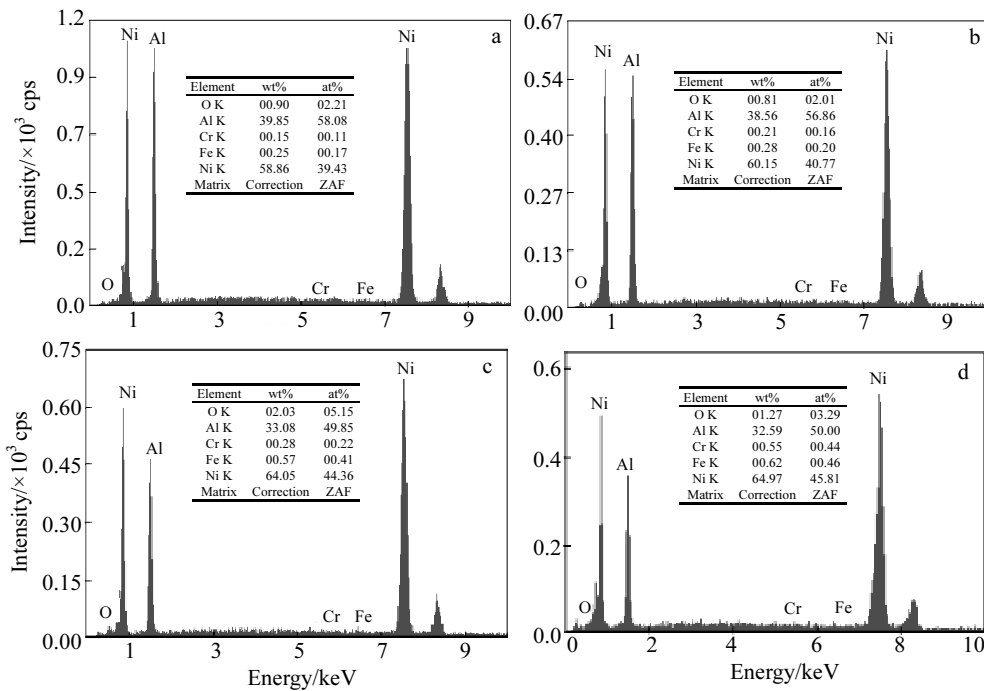Fig.6   X-ray diffraction pattern of surface of 1# coating with 2 wt% $CeCl_3$ oxidized at 650 °C for 132 h

Fig.7   EDS results of rare earth added Ni-Al composite coatings (sample 1#) at different oxidation time: (a) 24 h, (b) 60 h, (c) 96 h, and (d) 132 h

Table 2　Al/Ni atomic ratio of Ni-Al intermetallic at 650 °C

Ni-Al intermetallic	Al/Ni atomic ratio
Ni_2Al_3	1.43~1.71
NiAl	0.67~1.25
Ni_5Al_3	0.50~0.53
Ni_3Al	0.33~0.36

μm from the surface is $Ni_2Al_3 \rightarrow NiAl$. What's more, after a longer oxidation time (more than 132 h), phase transformation from NiAl to Ni_3Al may occur, which needs further study.

3　Conclusions

1) The addition of different contents of anhydrous $CeCl_3$ (2 wt%, 4 wt%, 6 wt%) to the aluminizing agent can improve the oxidation resistance of the coatings to varying degrees. After oxidization at 650 °C for 132 h, their oxidation kinetics curves all conform to the parabolic law, and the average oxidation rate for 2 wt%, 4 wt% and 6 wt% $CeCl_3$ contained coatings is 0.2957×10^{-6}, 0.3562×10^{-6} and 0.3533×10^{-6} g/(cm^2·s), respectively. The coating without rare earth has the fastest average oxidation rate of 0.4412×10^{-6} g/(cm^2·s).

2) Addition of a suitable amount of $CeCl_3$ (2 wt%) in the aluminizing agent can effectively retard the diffusion of Al. When the coating is oxidized at 650 °C for 132 h, Al can diffuse to a depth 38~41 μm to the coating surface.

3) The phase at 10 μm depth from the surface of the composite coating (2 wt% $CeCl_3$) begins to transform to NiAl at 650 °C at 60 h, and remains stable even with further extending the oxidation time to 132 h.

References

1　Hollner S, Fournier B, Pendu J L *et al*. *Journal of Nuclear Materials*[J], 2010, 405(2): 101

2　Výrostková A, Homolová V, Pecha J *et al*. *Materials Science & Engineering A*[J], 2008, 480(1-2): 289

3　Klueh R L. *Materials Reviews*[J], 2005, 50(5): 287

4　Taneike M, Abe F, Sawada K. *Nature*[J], 2003, 424(6946): 294

5　Żurek J, Wessel E, Niewolak L *et al*. *Corrosion Science*[J], 2004, 46(9): 2301

6　Kulevoy T V, Chalyhk B B, Fedin P A *et al*. *Review of Scientific Instruments*[J], 2016, 46(2): 411

7　Sánchez L, Bolívar F J, Hierro M P *et al*. *Intermetallics*[J], 2008, 16(10): 1161

8　Pint B A, Zhang Y, Walker L R *et al*. *Surface & Coatings Technology*[J], 2008, 202(4): 637

9　Pint B A, Zhang Y. *Materials & Corrosion*[J], 2015, 62(6): 549

10　Agüero A, Muelas R, Pastor A. *Surface & Coatings Technology*[J], 2005, 200(5-6): 1219

11　Xiang Z D, Rose S R, Datta P K. *Journal of Materials Science*[J], 2006, 41(22): 7353

12　Pint B A, Zhang Y, Walker L R *et al*. *Surface & Coatings Technology*[J], 2008, 202(4): 637

13　Zheng L, Peng X, Wang F. *Corrosion Science*[J], 2011, 53(2): 597

14　Wang J, Wu D J, Zhu C Y *et al*. *Surface & Coatings Technology*[J], 2013, 232: 489

15　Xiang Z D, Rose S R, Datta P K. *Intermetallics*[J], 2009, 17(6): 387

16　Xiang Z D, Datta P K. *Acta Materialia*[J], 2006, 54(17): 4453

17　Wang C, Li H, Zhang P *et al*. *Journal of Materials Engineering & Performance*[J], 2013, 22(2): 624

18　Prataap R K V, Mohan S. *Surface & Coatings Technology*[J], 2017, 324

19　Xu Jiawen, Liu Ailian, Wang Yongdong *et al*. *Rare Metal Materials & Engineering*[J], 2016, 45(6): 1413

20　Zhao Y T, Zhang S H, Ding Y *et al*. *Chinese Rare Earths*[J], 2015, 36(5): 92 (in Chinese)

21　Wagner C. *The Journal of Chemical Physics*[J], 1951, 19(5): 626

22　Zhang W, Wen J B, Long Y Q *et al*. *Transactions of Materials & Heat Treatment*[J], 2005, 25(6): 96

23　Domínguez-Crespo M A, Rodil S E, Torres-Huerta A M *et al*. *Surface & Coatings Technology*[J], 2009, 204(5): 571

24　Zhang W, Fan Z K, Guo X J *et al*. *Journal of Aeronautical Materials*[J], 2006, 26(2): 16

25　Li M, Li N, Zhang J *et al*. *Surface & Coatings Technology*[J], 2018, 337: 68

26　Karunaratne M S A, Carter P, Reed R C. *Materials Science & Engineering A*[J], 2000, 281(1): 229

27　Shankar S, Seigle L L. *Metallurgical Transactions A*[J], 1978, 9(10): 1467

28　Tanaka S. *Journal of the Electrochemical Society*[J], 2000, 147(147): 2242

29　Shi D, Wen B, Melnik R *et al*. *Journal of Solid State Chemistry*[J], 2009, 182(10): 2664

稀土 CeCl₃ 对耐热钢 Ni₂Al₃/Ni 复合涂层抗氧化性的影响

赵勇桃 [1]，田志华 [1]，李波波 [1]，任慧平 [2]

(1. 内蒙古科技大学，内蒙古 包头 014010)

(2. 内蒙古自治区白云鄂博矿多金属资源综合利用重点实验室，内蒙古 包头 014010)

摘　要： 采用电镀镍、低温包埋渗铝法在 P92 铁素体耐热钢表面制备不同稀土 Ce 含量的 Ni-Al 化合物复合涂层，并对复合涂层进行 650 °C/132 h 的抗氧化实验。利用 OM、SEM、EDS、XRD 分析涂层氧化前后的截面微观形貌，化学元素分布及物相变化规律。结果表明：涂层的氧化动力学曲线均符合抛物线规律。不含 Ce 的复合涂层平均氧化速率为 0.4412×10^{-6} g/(cm²·s)，渗铝剂中加入质量分数 2% CeCl₃ 的涂层抗氧化性明显增强，平均氧化速率为 0.2957×10^{-6} g/(cm²·s)，而加入过量 CeCl₃（4%、6%）则会在氧化过程中产生更多的孔洞，恶化涂层的高温抗氧化性能，氧化速率相对加入 2% CeCl₃ 的涂层有所升高。另外涂层中加入 Ce 元素增加了氧化膜的粘附性，对 Al 元素的向内扩散具有抑制作用。

关键词： Ni-Al涂层；P92钢；高温抗氧化性；Ce；电镀